Int. J. Nano Dimens., 10 (3): 297-303, Summer 2019

ORIGINAL ARTICLE

Electromagnetic absorption and structural properties of $SrFe_{11.98}Mg_{0.1}Sn_{0.1}O_{19}/BaTiO_3$ nanocomposites

Kameliya Ghaffarzadeh[1], Pirouz Derakhshi [1], Mohammad Yousefi [2,], Ali Mahmoudi [1], Parviz Aberoomand Azar [3]*

[1] *Department of Chemistry, Tehran North Branch, Islamic Azad University, Tehran, Iran.*
[2] *Department of Chemistry, Yadegar-e-Imam Khomeini (RAH) Shahre Rey Branch, Islamic Azad University, Tehran, Iran.*
[3] *Department of Chemistry, Science and Research Branch, Islamic Azad University, Tehran, Iran.*

Received 15 November 2018; revised 26 January 2019; accepted 07 February 2019; available online 19 February 2019

Abstract

In this research, first, nanoparticles of $SrFe_{11.98}Mg_{0.1}Sn_{0.1}O_{19}$ hexaferrite was synthesized via sol-gel auto-combustion process and then the nanocomposites of hexagonal ferrites/perovskite with the amounts of $SrFe_{11.98}Mg_{0.1}Sn_{0.1}O_{19}/BaTiO_3$ (50/50, 40/60, 70/30 w/w) was prepared by the ball-milling method. Fourier transform infrared (FTIR) spectrums of $SrFe_{11.98}Mg_{0.1}Sn_{0.1}O_{19}$, was shown that the bands at about 400 and 500 cm^{-1} proved the formation of nano hexagonal ferrites. On the FTIR spectrum of nanocomposites, the Ti-O bond of perovskite appeared. X-ray diffraction (XRD) analysis was confirmed the formation of hexaferrite and perovskite phase of $BaTiO_3$. Field emission electron microscopy (FESEM) pictures have represented the formation of hexagonal nanoparticles and sphere shape of $BaTiO_3$. Vibrating sample magnetometer (VSM) hysteresis loop was revealed that $SrFe_{11.98}Mg_{0.1}Sn_{0.1}O_{19}$ belonged to the soft magnetic materials due to the 604.45Oe coercivity. By formation of nanocomposites, the coercivity was increased up to 1500 Oe. Vector network analyzer (VNA) analysis was revealed the maximum absorption of -16.4 db at 11.5 GHz frequency for $SrFe_{11.98}Mg_{0.1}Sn_{0.1}O_{19}/BaTiO_3$ (60/40) nanocomposite sample.

Keywords: *Ball- Milling, Coercivity, Hexaferrite, Perovskite, Vector Network Analyzer.*

How to cite this article

Ghaffarzadeh K, Derakhshi P, Yousefi M, Mahmoudi A, Aberoomand Azar P. Electromagnetic absorption and structural properties of $SrFe_{11.98}Mg_{0.1}Sn_{0.1}O19/BaTiO_3$ nanocomposites. Int. J. Nano Dimens., 2019; 10 (3): 297-303.

INTRODUCTION

By using various kinds of magnetoelectronic devices, electromagnetic radiation interference results in human health damage and disclosure of information. As the result, electromagnetic absorber materials (EMA) have been developed in recent years [1-3]. M-Type hexaferrites with high Curie temperature, high electrical resistivity, and large magnetocrystalline anisotropy are the perfect candidate to be used as EMA materials [4, 5]. Till now, single compounds like M-type hexaferrites can't be prosperous in fulfilling all properties that ideal EMA (like maximum electromagnetic attenuation, and easy fabrication process) should have; however, composite materials act impressively [6]. On the other hand, for maximizing the attenuation of the electromagnetic wave, the electric and magnetic parts of absorber should be matched with each other [7]. Nanocomposites with two different phases of magnetic and dielectric materials can fulfill the goal of maximum attenuation and excellent impedance matching[8]. Hence, the new kinds of composites were synthesized by hexaferrites and the materials with large dielectric constant such as perovskite was added to maximize the attenuation of electromagnetic wave[9].

For obtaining beneficial electromagnetic absorber materials, a series of nanocomposites such as $SrFe_{12}O_{19}/NiFe_2O_4$ [10], $Fe–Sr_{0.8}La_{0.2}Fe_{11.8}Co_{0.2}O_{19}$

* Corresponding Author Email: myousefi50@hotmail.com

This work is licensed under the Creative Commons Attribution 4.0 International License.
To view a copy of this license, visit http://creativecommons.org/licenses/by/4.0/.

Archive of SID

www.SID.ir

[11], graphene/Strontium hexaferrite [12] and $(Ni_{0.65}Zn_{0.35}Fe_2O_4)_{0.85}$-$(BaFe_{12}O_{19})_{0.15}$ [13], was synthesized. Consequently, electromagnetic properties of nanocomposites were enhanced in comparison to the pure nanoparticles.

In this paper, $SrFe_{11.98}Mg_{0.1}Sn_{0.1}O_{19}/BaTiO_3$ (50/50, 40/60, 70/30 w/w) nanocomposites, for comparing microwave absorption properties have been synthesized via ball- milling method. First of all, $SrFe_{11.98}Mg_{0.1}Sn_{0.1}O_{19}$ was prepared by sol-gel auto combustion method. Then $BaTiO_3$ was fabricated by the sol-gel method. Finally, nanocomposites of $SrFe_{11.98}Mg_{0.1}Sn_{0.1}O_{19}/BaTiO_3$ (50/50, 40/60, 70/30 w/w) was provided by ball- milling process. All the samples were characterized by FTIR (fourier transform infrared), XRD (x-ray diffraction), FESEM (field emission electron microscopy) and VSM (vibrating sample magnetometer) analysis. The absorption properties of each sample were investigated by VNA (vector network analyzer).

METHODS AND MATERIALS

An analytical grade of $Sr(NO_3)_2$, $Fe(NO_3)_3$, $Mg(NO_3)_2$, $SnCl_4$, $Ba(NO_3)_2$, Lucien, tetra-n-butyl titanate, citric acid, ammonium hydroxide, was used without further purification.

$SrFe_{11.98}Mg_{0.1}Sn_{0.1}O_{19}$ synthesis

$SrFe_{11.98}Mg_{0.1}Sn_{0.1}O_{19}$ was synthesized with sol-gel auto-combustion method. $Sr(NO_3)_2$, $Fe(NO_3)_3$, $Mg(NO_3)_2$, $SnCl_4$ and citric acid was dissolved in 400mL deionized water. The solution was heated up to 100°C, and then by ammonia solution adding the pH was reached to 8. Gradually the sol was ignited and converted to a viscous gel. Finally, auto-combustion happened. The powder was calcined at 900°C for 5 hours [14].

$BaTiO_3$ synthesis

0.25g barium nitrate and 0.3g Lucien was dissolved in distilled water. 0.5ml tetra-n-butyl titanate was added into the solution under vigorous stirring. The gel was obtained at 100°c and calcined at 700°c [15].

$SrFe_{11.98}Mg_{0.1}Sn_{0.1}O_{19}/BaTiO_3$ nanocomposite synthesis

Stoichiometric amounts of $SrFe_{11.98}Mg_{0.1}Sn_{0.1}O_{19}$ and $BaTiO_3$ was weighted and mortgaged. The certain weight ratio (50/50, 40/60, 70/30) of samples was a ball- milled for 36h. The samples were dried at the vacuumed oven.

Preparing samples for microwave absorption

Preparation of samples for electromagnetic absorption measurements was accomplished by mixing nanocomposites with paraffin (mass ratio70/30). The samples were molded in the rectangular template with 22.86×10.16×1mm diameter and 3mm thickness.

Characterization

(Model: XPERT-MPD, Philips) with Cu Kα radiation (λ=1.5418Å) over the 2Θ rang of 10-80° with a step rate of 5°/min. Field emission scanning electron (SIGMA, VP-500, ZEISS model), was utilized for estimating morphology of samples. The magnetic properties of samples were characterized by Lake Shore7307 vibrating sample magnetometer. Microwave absorption in the range of X bands frequency was calculated with a vector network analyzer (VNA, Agilent 8510C).

RESULTS AND DISCUSSIONS

FTIR spectrums

The FTIR spectrum of $SrFe_{11.98}Mg_{0.1}Sn_{0.1}O_{19}$ and $SrFe_{11.98}Mg_{0.1}Sn_{0.1}O_{19}/BaTiO_3$ (50/50, 40/60, 70/30 w/w) nanocomposites was shown at Fig. 1(a-d). FTIR spectrum, implying the preparation processes of FTIR. In pure $SrFe_{11.98}Mg_{0.1}Sn_{0.1}O_{19}$ nanoparticles, show the peaks at 423.12 and 582. 48cm^{-1} was related to the vibration of the Fe-O bond at tetrahedral and octahedral vibrations (Fig.1a) [16]. In $SrFe_{11.98}Mg_{0.1}Sn_{0.1}O_{19}/BaTiO_3$ nanocomposite, besides hexaferrite vibrating modes (550, 549.62 and 547.39 cm^{-1}), the new bands at 589.03, 590.01 and 592.0.5 cm^{-1} correspond to the vibration of Ti-O octahedron of perovskite structure (fig 1b, 1c, and 1d). [17].

XRD results

The XRD patterns of samples were presented at Fig. 2(a-d). XRD patterns reveal that the formation of Strontium hexaferrite which was matched with the JCPDS number 98-004-3590. The crystallite size of particles was calculated by Scherer's equation (1):

$$D = 0.9\lambda B\cos\theta \quad (1)$$

In which λ is the X-ray wavelength, B is the full width at half maximum and θ is the diffraction angle. The average crystallite size of $SrFe_{11.98}Mg_{0.1}Sn_{0.1}O_{19}$ is about 89 nm. The peaks with Miller indices of (110), (107), (114), (108),

Archive of SID

www.SID.ir

(203), and (205) presented the formation of strontium hexagonal ferrite [18].

In X-ray patterns of $SrFe_{11.98}Mg_{0.1}Sn_{0.1}O_{19}/BaTiO_3$ (50/50, 40/60, 70/30 w/w) nanocomposites, the peaks which were related to the hexaferrite (cycles) and perovskites (stars) was appeared in Fig. 2b, 2c and 2d. This kind of X-ray patterns shows that the nanocomposites of hexaferrite/perovskites were synthesized successfully [19]. There were no impurities in XRD results which was represented by the formation of pure nanocomposites.

FESEM pictures

FESEM micrographs of samples were shown at Fig. 3 (a-d). Hexagonal platelet structure of $SrFe_{11.98}Mg_{0.1}Sn_{0.1}O_{19}$ reveals the formation of hexaferrite (Fig. 3a). In $SrFe_{11.98}Mg_{0.1}Sn_{0.1}O_{19}/BaTiO_3$ nanocomposites, the spherical particles of $BaTiO_3$ and hexagonal structure of $SrFe_{11.98}Mg_{0.1}Sn_{0.1}O_{19}$ confirm the existence of nanocomposites (Fig. 3b, 3c, and 3d). In all products agglomeration of samples was happened due to magnetic properties of M-type hexagonal ferrites [20-23].

VSM hysteresis loops

Hysteresis loops of $SrFe_{11.98}Mg_{0.1}Sn_{0.1}O_{19}$ and $SrFe_{11.98}Mg_{0.1}Sn_{0.1}O_{19}/BaTiO_3$ (50/50, 40/60, 70/30 w/w) nanocomposites was represented at Fig. 4 (a-d). Iron in the hexagonal structure occupied five different sites in tetrahedral $4f_1$ (↓), bipyramidal

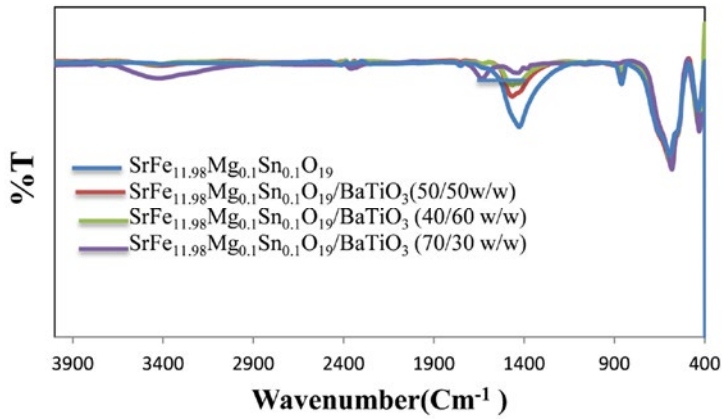

Fig. 1. FTIR - $SrFe_{11.98}Mg_{0.1}Sn_{0.1}O_{19}$, - $SrFe_{11.98}Mg_{0.1}Sn_{0.1}O_{19}/BaTiO_3$ (50/50w/w), - $SrFe_{11.98}Mg_{0.1}Sn_{0.1}O_{19}/BaTiO_3$ (40/60 w/w), - $SrFe_{11.98}Mg_{0.1}Sn_{0.1}O_{19}/BaTiO_3$ (70/30 w/w).

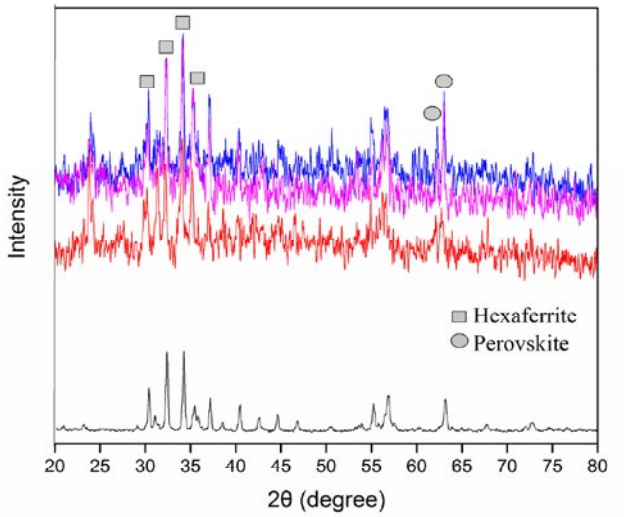

Fig. 2. XRD -$SrFe_{11.98}Mg_{0.1}Sn_{0.1}O_{19}$, - $SrFe_{11.98}Mg_{0.1}Sn_{0.1}O_{19}/BaTiO_3$ (50/50w/w), - $SrFe_{11.98}Mg_{0.1}Sn_{0.1}O_{19}/BaTiO_3$ - $SrFe_{11.98}Mg_{0.1}Sn_{0.1}O_{19}/BaTiO_3$ (70/30 w/w).

www.SID.ir

2b (↑), and three octahedral sites (12 K (↑), $4f_2$ (↓), and2a (↑)) [24]. On the whole, 4+ cation is responsible for the magnetization properties of samples[25]. Sn^{4+} is substituted for Fe^{3+} in bipyramidal 2b and tetrahedral $4f_1$ sites. For more distortion, tin preferred to occupy bipyramidal 2b rather than $4f_1$ sites [26]. As a result, the saturation magnetization decreased in comparison to the pure strontium hexaferrite (56emu/g) [27]. In $SrFe_{11.98}Mg_{0.1}Sn_{0.1}O_{19}/BaTiO_3$ nanocomposites by adding $BaTiO_3$, saturation magnetization reduced (39.81 to 28.83 emu/g) due to the non-magnetic properties of perovskites. In 60/40 and 70/30 nanocomposites because of the increasing of magnetic phase (hexaferrite), the saturation magnetization increased (35.34 and 36.14 emu/g) (Fig. 4b, 4c, and 4d). Magnetic data of all samples was observed at Table 1. The coercivity of doped strontium hexaferrite was decreased (5000Oe to 604.45Oe) due to the improvement of uniaxial anisotropy along the *c* axis. Based on equation (2):

$$H_c = 2k / \mu_0 M_s \qquad (2)$$

In which coercivity is in reverse relation with saturation magnetization. In this equation K is magnetocrystalline anisotropy constant, M_S is the saturation magnetization, m_0 is the permeability of free space and H_c is coercivity. By decreasing saturation magnetization from 39.81 to 28.83

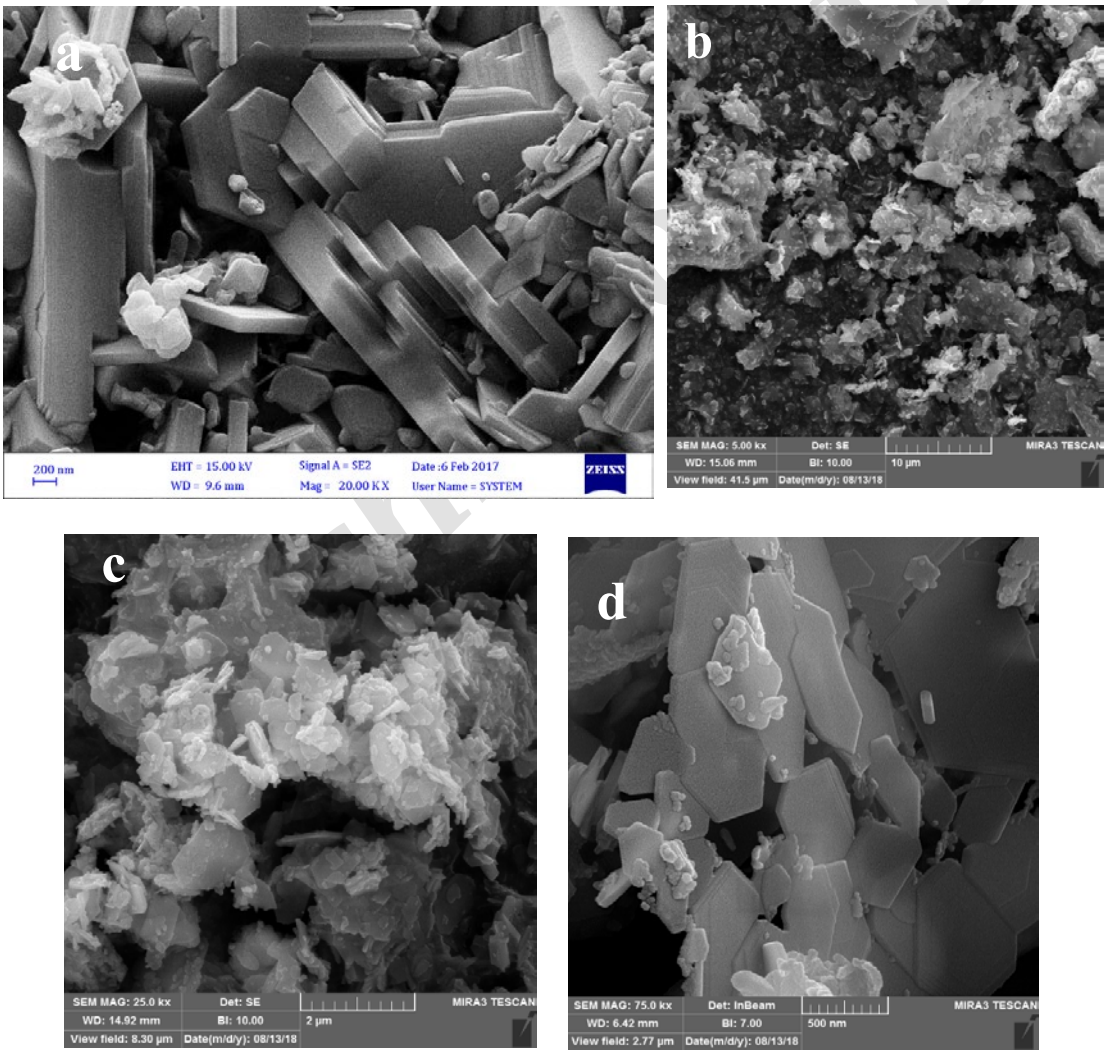

Fig. 3 (a-d). FESEM micrograph a) $SrFe_{11.98}Mg_{0.1}Sn_{0.1}O_{19}$, b) $SrFe_{11.98}Mg_{0.1}Sn_{0.1}O_{19}/BaTiO_3$ (50/50w/w), c) $SrFe_{11.98}Mg_{0.1}Sn_{0.1}O_{19}/BaTiO_3$ (40/60 w/w), d) $SrFe_{11.98}Mg_{0.1}Sn_{0.1}O_{19}/BaTiO_3$ (70/30 w/w).

www.SID.ir

emu/g, the coercivity was increased from 604.45 to 1500 Oe. The sequence ratio (M_r/M_s) of all samples was calculated. The various ratio of M_r/M_s differed each sample in a different application.

Electromagnetic absorption properties

Microwave absorption properties of samples were investigated by reflection loss, and the reflection loss can be calculated by following equation based on transmission loss theory (3):

$$R(db) = 20\log\left|\frac{z_{in}-1}{z_{in}+1}\right|$$

$$z_{in} = \sqrt{\frac{\mu_r}{\varepsilon_r}}\tanh\left[j\left(\frac{2\pi}{c}\right)\sqrt{\mu_r\varepsilon_r}fd\right] \quad (3)$$

In these equations, Z_{in} is the input impedance, μ_r is the permeability, ε_r is the permittivity, *f* is the microwave frequency, *c* is the light velocity, *d* is the thickness of absorbing layer and j is an imaginary number. The effective bandwidth describes the frequency with the reflection loss is less than -10 db [28]. In $SrFe_{11.98}Mg_{0.1}Sn_{0.1}O_{19}$ M-type hexaferrite, reflection loss is -4db at 8-12GHz range which reveals that the doped strontium hexaferrite shows the absorbance percentage of about 10% (Fig. 5). By adding perovskite, the reflection loss reaches to -16.4db at 11.5 GHz for $SrFe_{11.98}Mg_{0.1}Sn_{0.1}O_{19}/BaTiO_3$ 60/40 nanocomposite. In $SrFe_{11.98}Mg_{0.1}Sn_{0.1}O_{19}/BaTiO_3$ 50/50 nanocomposite, the reflection loss reaches to -16db at 12 GHz. In $SrFe_{11.98}Mg_{0.1}Sn_{0.1}O_{19}$/

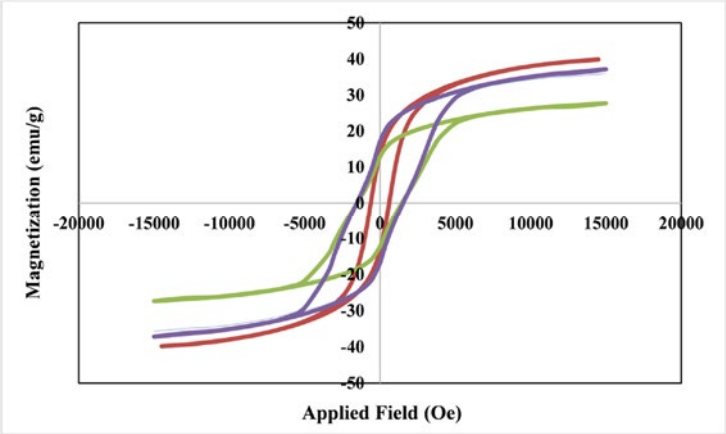

Fig. 4. Hysteresis loops of - $SrFe_{11.98}Mg_{0.1}Sn_{0.1}O_{19}$, -$SrFe_{11.98}Mg_{0.1}Sn_{0.1}O_{19}/BaTiO_3$ (50/50w/w), - $SrFe_{11.98}Mg_{0.1}Sn_{0.1}O_{19}/BaTiO_3$ (40/60 w/w), - $SrFe_{11.98}Mg_{0.1}Sn_{0.1}O_{19}/BaTiO_3$ (70/30 w/w).

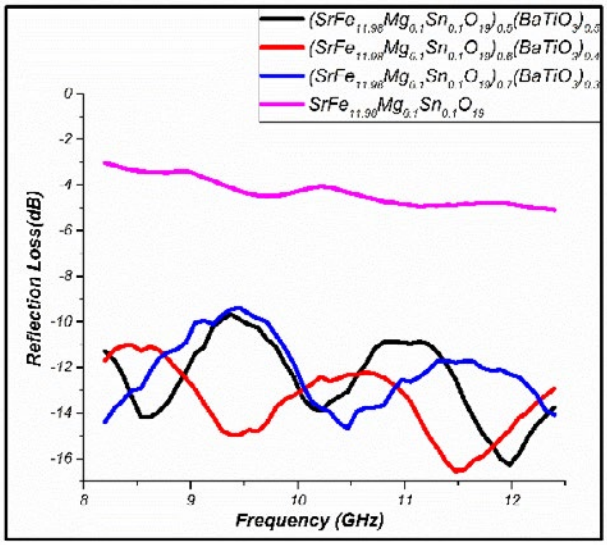

Fig. 5. Reflection loss versus frequency curves of $SrFe_{11.98}Mg_{0.1}Sn_{0.1}O_{19}$ and $SrFe_{11.98}Mg_{0.1}Sn_{0.1}O_{19}/BaTiO_3$ (50/50, 40/60, 70/30 w/w).

www.SID.ir

Table 1. Magnetic data of $SrFe_{11.98}Mg_{0.1}Sn_{0.1}O_{19}$ and $SrFe_{11.98}Mg_{0.1}Sn_{0.1}O_{19}/BaTiO_3$ (50/50, 40/60, 70/30 w/w).

sample	M_s(emu/g)	M_r(emu/g)	M_r/M_s	H_c(Oe)
$SrFe_{11.98}Mg_{0.1}Sn_{0.1}O_{19}$	39.81	35.14	0.88	604.45
$SrFe_{11.98}Mg_{0.1}Sn_{0.1}O_{19}/BaTiO_3$ (50/50)	28.83	23.69	0.82	1500
$SrFe_{11.98}Mg_{0.1}Sn_{0.1}O_{19}/BaTiO_3$(60/40)	35.34	32.21	0.91	1500
$SrFe_{11.98}Mg_{0.1}Sn_{0.1}O_{19}/BaTiO_3$(70/30)	36.14	32.77	0.90	1500

$BaTiO_3$ 70/30 nanocomposite the reflection loss reaches to -14.8db at 10.5GHz. The reports reveal that coupling dielectric loss and magnetic loss mechanism can improve the electromagnetic wave attenuation and consequently increase the reflection loss. Therefore, by adding $BaTiO_3$ to $SrFe_{11.98}Mg_{0.1}Sn_{0.1}O_{19,}$ rather than magnetic loss, the dielectric loss mechanism will be occurred on the surface of the nanocomposite due to the interfacial polarization. As a result, the reflection loss increases from -4 to -16.4db at GHz in 3mm thickness.

CONCLUSIONS

The $SrFe_{11.98}Mg_{0.1}Sn_{0.1}O_{19}/BaTiO_3$ nanocomposite was synthesized successfully. FTIR spectrums approve the formation of nanocomposites. XRD results show that both phases of hexaferrite and perovskite were synthesized completely. FESEM pictures represent the hexagonal structure of $SrFe_{11.98}Mg_{0.1}Sn_{0.1}O_{19}$ and sphere shape of $BaTiO_3$. By adding perovskite phase, the saturation magnetization of nanocomposites was decreased due to the reduction of magnetic hexaferrite phase. For adjusting, dielectric and magnetic parts of the electromagnetic absorber, the perovskite with high dielectric properties were added to the hexaferrite. After this adjustment, the reflection loss of the sample was enhanced.

CONFLICT OF INTEREST

The authors declare that there are no conflicts of interest regarding the publication of this manuscript.

REFERENCES

[1] Chen J., (2016), Electromagnetic and microwave absorption properties of $BaMg_xCo_{1-x}TiFe_{10}O_{19}$. *J. Alloys Comp.* 679: 335-340.

[2] Huang X., Chen Z., Tong L., (2013), Preparation and microwave absorption properties of $BaTiO_3$@MWCNTs core/shell heterostructure. *Mater.Lett.*111: 24-27.

[3] Zhang L., (2006), Preparation of PANI/TiO_2 nanocomposites and their solid-phase photocatalytic degradation. *Polym. Degrad. Stability.*91: 2213-2219.

[4] Pullar R. C., (2012), Hexagonal ferrites: A review of the synthesis, properties and applications of hexaferrite ceramics. *Prog. Mater. Sci.* 57: 1191-1334.

[5] Yanbing H., Sha J., Lina S., (2009), Tailored magnetic properties of Sm(Zn) substituted nanocrystalline barium hexaferrites. *J. Alloys Comp.* 486: 348-351.

[6] Hessien M. M., (2008), Controlling the composition and magnetic properties of strontium hexaferrite synthesized by co-precipitation method. *J. Magnetis.Magnet. Mater.*320:336-343.

[7] Luo J., Xu Y., Mao H., (2015), Magnetic and microwave absorption properties of rare earth ions (Sm^{3+}, Er^{3+}) doped strontium ferrite and its nanocomposites with polypyrrole. *J. Magnetis.Magnet. Mater.* 381: 365-371.

[8] Lee W. W., Chung W.-H., Huang W.-S., Lin W.-C., Jiang Y.-R., (2013),Photocatalytic activity and mechanism of nano-cubic barium titanate prepared by a hydrothermal method. *J. Taiwan Inst.Chem. Eng.* 44: 660-669.

[9] Afghahi S. S. S., Jafarian M., (2016), Microstructural and magnetic studies on $BaMg_xZn_xX_{2x}Fe_{12-4x}O_19$ (X=Zr,Ce,Sn) prepared via mechanical activation method to act as a microwave absorber in X-band. *J. Magnetis. Magnet. Mater.* 406: 184-191.

[10] Mehdipour M., (2013),Comparison of microwave absorption properties of $SrFe_{12}O_{19}$, $SrFe_{12}O_{19}/NiFe_2O_4$, and $NiFe_2O_4$ particles. *J. Appl. Phys.*114: 420-427.

[11] Zhang Z., (2012), Electro magnetic and microwave absorption properties of $Fe–Sr_{0.8}La_{0.2}Fe_{11.8}Co_{0.2}O_{19}$ shell-core composites. *J. Magnetism. Magnet. Mater.*324: 2177-2182.

[12] Durmus Z., Kavas H., (2015), Synthesis and micro-structural characterization of graphene/strontium hexaferrite ($SrFe_{12}O_{19}$) nanocomposites. *Mater. Chem. Phys.*163: 439-445.

[13] Subhenjit Hazra B. K. G., Kumar Patra M., (2015), A novel 'One-Pot' synthetic method for preparation of $(Ni_{0.65}Zn_{0.35}Fe_2O_4)_x$-$(BaFe_{12}O_{19})_{1-x}$ nanocomposites and study of their microwave absorption and magnetic properties. *Powder Technol.* 279: 10-17.

[14] Khorrami S., Gharib F., (2011), Synthesis and characterization of nanocrystalline spinel Zinc ferrite prepared by sol-gel auto-combustion technique. *Int. J. Nano Dimens*. 3: 221-224.

[15] Enhessari M., Nazari Moghadam S., (2010), Synthesis and characterizations of $CoTiO_3$-clay nanocomposites by sol-gel method. *Int. J. Nano Dimens.* 2: 125-232.

[16] Mosleh Z., Kameli P., Poorbaferani A., Ranjbar M., (2016), Structural, magnetic and microwave absorption properties of Ce-doped barium hexaferrite. *J. Magnetis. Magnet. Mater.* 397: 101-107.

[17] Sun D., Jin X., (2007), Investigation on FTIR spectrum of bariumtitanate ceramics doped with alkali ions. *Ferroelectrics.* 355: 145-148.

[18] Iqbal M. J., (2017), Physical, electrical and dielectric properties of Ca-substituted strontium hexaferrite ($SrFe_{12}O_{19}$) nanoparticles synthesized by co-precipitation

Archive of SID

www.SID.ir

method. *J. Magnetis. Magnet. Mater*. 322: 1720-1726.
[19] Ozah S., Bhattacharyya N. S., (2015), Development of BaAlxFe12−xO19-NPR nanocomposite as an efficient absorbing material in the X-band. *J. Magnetis. Magnet. Mater.* 374: 516-524.
[20] Wang L., (2014), Magnetic and microwave absorption properties of $BaMn_xCo_{1-x}TiFe_{10}O_{19.}$ *J. Alloys Comp.* 588: 2012-216.
[21] wang L., (2015), XAFS and XPS studies on site occupation of Sm^{3+} ions in Sm doped M-type $BaFe_{12}O_{19}$. *J. Magnetis. Magnet. Mater.* 377: 362-367.
[22] Wang H. Z., Yao B., (2012), Improvement of the coercivity of strontium hexaferrite induced by substitution of Al^{3+} ions for Fe^{3+} ions. *J. Alloys Comp.* 537: 43-49.
[23] Wang J., Ponton C., (2005). A study of Pr-substituted strontium hexaferrite by hydrothermal synthesis. *J. Alloys Comp.* 403: 104-109.
[24] Chawla S., Mudsainiyan R., Meena S., (2014), Sol–gel synthesis, structural and magnetic properties of nanoscale M-type barium hexaferrites $BaCo_xZr_xFe_{(12-2x)}O_{19}$. *J. Magnetis. Magnet. Mater.* 350: 23-29.
[25] Mousavinia M., Ghasemi A., (2014), Structural, magnetic, and reflection loss characteristics of Ni/Co/Sn-substituted strontium ferrite/functionalized MWCNT nanocomposites. *J. Elec. Mater.*43: 2573-2583.
[26] Ghezelbash S., Yousefi M., Hossainisadr M., Baghshahi S., (2018), Structural and magnetic properties of Sn^{4+} doped strontium hexaferrites prepared via sol–gel auto-combustion method. *IEEE Transac. Magnet.* 54: Article Sequence Number: 2001306.
[27] Sharbati A., (2012), Microwave absorption studies of nanocrystalline $SrMn_{x/2}(TiSn)_{x/4}Fe_{12-x}O_{19}$ prepared by the citrate sol–gel method. *Solid State Communic.* 152: 199-203.
[28] li J., (2012), Preparation, magnetic and electromagnetic properties of polyaniline/strontium ferrite/multiwalled carbon nanotubes composite. *Appl. Surf. Sci.* 258: 3659-3666.

Archive of SID

(cc) BY

www.SID.ir